Vibration Analysis of Composite Horizontal

Cylindrical Tank with Different Layering using the Finite Element Method

Hossein Farahani^{1*}, Farzan Barati² and Hamid Batmani³

Department of Mechanical Engineering, Hamedan Branch, Islamic Azad University, Hamedan, Iran; farahani.h63@gmail.com

²Department of Mechanical Engineering, Hamedan Branch, Islamic Azad University Hamedan, Iran ³Department of Mechanics, College of Engineering, Hamedan Science and Research Branch, Islamic Azad University, Hamedan, Iran

Abstract

This paper focuses on the vibration analysis of composite cylindrical tank. The purpose of this study is comparison of natural frequencies with different layering and different fiber angle along the x-axis of the tank. The boundary conditions of the tank are located at the beginning and the end of tank. The tank fixed along the coordinate system (y, z) and is free in x-axis. Stability equations derived using the first-order shear deformation theory. The effect of layering and fiber angle has evaluated by using the finite element package ANSYS. The angle considered between -90 to 90 degrees also 0 to 90 degrees for position of fibers along the thickness, which distributed in the form of symmetrical and asymmetric. Finally, the natural frequencies of the tank under the effect of layering of composite in radial direction compared. The results shown that the number of layers and fiber orientation affected on the natural frequencies.

Keywords: Cylindrical Tank, Composite, Finite Element, Natural Frequencies

1. Introduction

Cylindrical tanks with different shape and size are used in the chemical and petrochemical industries. Among the different types of shells, cylindrical shells are particular importance. Researchers have been trying to changes on the sidewall and material of these shells to increase their resistance against the load and decrease their weight. Variety of tanks that used in different industries has caused that design and installation of these reservoirs is very important. In the recent researches, El Damatty et al.1 developed a numerical model to predict the dynamic response of flexible conical tanks. The model was based on a coupled shell-boundary element theory with assumption of decoupling between the sloshing component and the shell.

Dynamic behavior of three models of steel cylindrical reservoirs containing fluid modeled using ANSYS software with applying the finite element method is studied by Mansouri and Aminnejad². In this modeling, features of a cylindrical reservoir containing 0.9 height of liquid is used which its fluid is considered to be incompressible and viscose. Sweedan and El Damatty³ carried out some experiments to identify the vibration modes of liquid-filled conical tanks. Amabili4-6 performed some theoretical and experimental works on the nonlinear vibrations of fluid-filled cylindrical tanks and analyzed the effects of boundary conditions, large deformations and imperfection on the dynamic characteristics of the tank. Recently, Karagiozis et al.7 investigated the nonlinear vibrations of fluid-filled clamped circular cylindrical shells. Also, Zhou and Liu⁸ studied the three-dimensional vibratory characteristics of flexible rectangular tanks partially filled with fluid using an analytical solution. In the field of fluid-structure interaction in composite

tanks, there are relatively newer research works. Dehghan Manshadi and Maheri9 are presented the results of numerical investigations on the effects of material degradation due to corrosion on the dynamic characteristics of ground-based, anchored, steel liquid storage tanks. Internal corrosion is considered as a time-dependent constant thinning of the wall, at locations in contact with residual water, water condensate, atmospheric oxygen and acid gases. Pal et al. 10 made a study on the sloshing dynamics in a fluid-filled laminated composite open cylindrical tank and later accomplished their work assuming nonlinear free surface boundary conditions using finite element method. Larbi et al.¹¹ presented the theoretical and finite element formulations of piezoelectric composite shells of revolution filled with compressible fluid. In the present study, the finite element method along with the modal analysis technique used to derive the equations governing the structural dynamics of the laminated composite tank. The dynamic behavior of cylindrical open top groundsupported water tanks is investigated by Moslemi and Kianoush¹². The main focus of this study is to identify the major parameters affecting the dynamic response of such structures and to address the interaction between these parameters.

In this study, the vibration of the cylindrical tank used in the industry is examined. To obtain the equilibrium equations used the First order Shear Deformation Theory (FSDT). The tank is made of graphite-epoxy. Obtain the natural frequencies of the tank, trying to not equal frequency of stimulating forces and frequency for does not occur resonance, is the purpose of this study. To finding the effect of different layering, the wall of cylindrical tank has been divided into several layers in the radial direction and the material properties of each layer is assumed to be constant. The tank has been considered to three-layer composite and six-layer composite and finally with comparing of these cases we offer the best layering.

2. Equilibrium Equations

Consider a composite cylindrical tank which has a constant thickness h, radius R and length L as shown in Figure 1 that the thermal and mechanical properties are changed along the thickness of the tank continuously. Throughout the current investigation x, y and z coordinates coincide that x coordinate is taken in the axial direction of the shell.

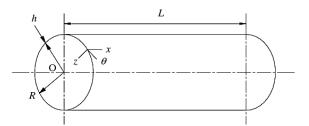


Figure 1. Coordinate system of cylindrical tank.

The material distribution governed by the equation:

$$V = (V_{out} - V_{in}) \left(\frac{r - r_{in}}{r_{out} - r_{in}} \right) + V_{in}$$
 (1)

Where V, is the volume fraction of material constituent, V_{in} and V_{out} , is the effect of external and internal surfaces of Tank, and n is an exponential distribution coefficient. Thin-walled cylinders assumed with finite length and the mechanical and thermal loads are axial symmetry conditions. Thus can regardless of θ in equations. Therefore, the equilibrium equations written as:

$$\frac{1}{r}\frac{\partial(r\sigma_r)}{\partial r} - \frac{\sigma_{\theta}}{r} + \frac{\partial\sigma_{rz}}{\partial z} = \rho \frac{\partial^2 u_r}{\partial t^2}, \quad \frac{1}{r}\frac{\partial(r\sigma_{rz})}{\partial r} + \frac{\partial\sigma_z}{\partial z} = \rho \frac{\partial^2 u_z}{\partial t^2}$$
(2)

$$\varepsilon_{r} = \frac{\partial u_{r}}{\partial r}, \ \varepsilon_{\theta} = \frac{u_{r}}{r}, \ \varepsilon_{z} = \frac{\partial u_{z}}{\partial z}$$

$$\gamma_{r\theta} = \frac{\partial u_{\theta}}{\partial r} - \frac{u_{\theta}}{r}, \ \gamma_{rz} = \frac{\partial u_{z}}{\partial r} - \frac{\partial u_{r}}{\partial z}, \ \gamma_{\theta z} = \frac{\partial u_{\theta}}{\partial z}$$
(3)

Where, u_r , u_θ and u_z are displacements of arbitrary points through the cylindrical tank along coordinates (x, y, z). The relationships of stress - strain in three-dimensional defined as:

$$\begin{cases}
\sigma_Z \\
\sigma_\theta \\
\sigma_r
\end{cases} =
\begin{bmatrix}
C_{11} & C_{12} & C_{12} \\
C_{12} & C_{11} & C_{12} \\
C_{12} & C_{12} & C_{11}
\end{bmatrix}
\begin{pmatrix}
\varepsilon_z \\
\varepsilon_\theta \\
\varepsilon_r
\end{pmatrix} -
\begin{pmatrix}
a \\
a \\
a
\end{pmatrix} \Delta T$$
(4)

Where, ΔT is the temperature (K) and C_{ij} (i = 1, 2) are the reduced stiffnesses, and for isotropic materials they are expressed as:

$$C_{11} = \frac{E(1-\nu)}{(1+\nu)(1-2\nu)}, \ C_{12} = \frac{E\nu}{(1+\nu)(1-2\nu)}, \ C_{66} = (C_{11} - C_{12})/2$$
(5)

In the above relations $\sigma_i(i=z, \theta, r)$, ε_i represent the normal stress components, normal strain components respectively.

Considering the boundary conditions u_{θ} is zero and can solve the problem in (r, z). Substituting the Eq. (3) in Eq. (4), relationships of stress - displacement obtained as:

$$\sigma_{z} = C_{11} \frac{\partial u_{z}}{\partial z} + C_{12} \left(\frac{u_{r}}{r} + \frac{\partial u_{r}}{\partial r} \right) - \sigma_{T}$$

$$\sigma_{\theta} = C_{11} \frac{u_{r}}{r} + C_{12} \left(\frac{\partial u_{z}}{\partial z} + \frac{\partial u_{r}}{\partial r} \right) - \sigma_{T}$$

$$\sigma_{r} = C_{11} \frac{\partial u_{r}}{\partial r} + C_{12} \left(\frac{u_{r}}{r} + \frac{\partial u_{z}}{\partial z} \right) - \sigma_{T}$$

$$\sigma_{r\theta} = C_{66} \left(\frac{\partial u_{\theta}}{\partial r} - \frac{u_{\theta}}{r} \right), \quad \sigma_{rz} = C_{66} \left(\frac{\partial u_{z}}{\partial r} + \frac{\partial u_{r}}{\partial z} \right),$$

$$\sigma_{\theta z} = C_{66} \left(C_{11} + 2C_{12} \right) \tag{6}$$

Where:

$$\sigma_T = a\Delta T (C_{11} + 2C_{12}) \tag{7}$$

Whit substituting Eq. (6) in the elastic equilibrium equation (Eq. (2)) the coupled differential equations obtained as:

$$\frac{1}{r}\frac{\partial}{\partial r}\left(C_{11}r\frac{\partial u_r}{\partial r} + C_{12}\left(u_r + r\frac{\partial u_z}{\partial z}\right) - r\sigma_T\right) \\
-C_{11}\frac{u_r}{r^2} + \frac{\partial}{\partial z}\left(C_{66}\left(\frac{\partial u_z}{\partial r} + \frac{\partial u_r}{\partial z}\right)\right) \\
-\frac{C_{12}}{r}\left(\frac{\partial u_r}{\partial r} + \frac{\partial u_z}{\partial z}\right) + \frac{\sigma_T}{r} = 0 \\
\frac{\partial}{\partial z}\left(C_{11}\frac{\partial u_z}{\partial z} + C_{12}\left(\frac{u_r}{r} + \frac{\partial u_r}{\partial r}\right) - \sigma_T\right) \\
-\frac{1}{r}\frac{\partial}{\partial r}\left(C_{66}r\left(\frac{\partial u_z}{\partial r} + \frac{\partial u_r}{\partial z}\right)\right) = 0 \tag{8}$$

Based on this definition, the matrix form of the equilibrium equations and the related boundary conditions by using interpolation functions (ψ) becomes:

$$u_r = \sum_{j=1}^{n_c} u_j \psi_j, \ u_z = \sum_{j=1}^{n_c} v_j \psi_j, \ w_1 = w_2 = \psi_i$$
 (9)

The final equations Equilibrium obtained as:

$$\begin{bmatrix} k_{bb} & k_{bd} \\ k_{db} & k_{dd} \end{bmatrix} \begin{Bmatrix} u \\ v \end{Bmatrix} = \begin{Bmatrix} F_1 \\ F_2 \end{Bmatrix} + \begin{Bmatrix} Q_1 \\ Q_2 \end{Bmatrix}$$
 (10)

Where, b and d correspond to the displacement vectors at the boundaries and domain of the shell, respectively.

Please see the Appendix. 1.

3. Finite Element Modeling

3.1 Material

The basic materials properties determined are displayed in Table 1

The SOLID46 element in the finite element package ANSYS used for modeling and analysis of composite materials. The cylindrical tank has spherical lenses that these lenses have tow radius. Three-dimensional model of the tank is shown in Figure 2.

Table 1. The mechanical properties of composite

Mechanical properties	Graphite - epoxy
v_{23}	0.458
v_{13}	0.248
$v_{_{12}}$	0.248
$lpha_{_1}$	$-0.018*10^{-60}$ C
$lpha_{_2}$	24.3*10 ⁻⁶ °C
$lpha_{_3}$	24.3*10 ⁻⁶ °C
$oldsymbol{eta}_{_1}$	$146*10^{-6} \%M$
$oldsymbol{eta}_{\!\scriptscriptstyle 2}$	$4770^*10^{-6} \%M$
$oldsymbol{eta}_{_3}$	4770*10 ⁻⁶ %M
ho	1540Kg/m^3
$\mathbf{E}_{_{1}}$	155GPa
$\mathrm{E_2}$	12.1GPa
$\mathrm{E}_{_{3}}$	12.1 GPa
G_{12}	4.4 GPa
G_{13}	4.4 GPa
G_{23}	3.2 GPa
S	100MPa
X_c	-1250 MPa
X_{t}	1500 MPa
Y_c	-200 MPa
Y_t	50 MPa

The cylindrical tank properties are as follows: The Length of cylindrical: 2.5m

Outer diameter of the cylindrical: 1m

Thickness of the cylindrical shell: 20*10-3m

Knuckle radius of the lens: 0.18m

Knuckle angle of lens: 60°

Internal form of the lens radius: 0.88m

3.2 Boundary Conditions

Figure 3 shown the boundary conditions of the tank that one bases fixed and another base fixed in directions *y* and *z* coordinates.

We've meshed the model, after determining the properties of the used material. The elements should considered along the thickness of the tank. Figure 4. illustrates the thickness in direction of an element.

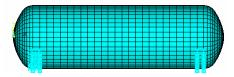


Figure 2. Three-dimensional of the tank model.

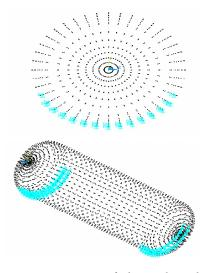


Figure 3. Isometric scene of the tank with boundary conditions.



Figure 4. The thickness in direction of an element.

The fundamental mode shapes of vibration for intended tank are shown in Figure 5.

3.3 Composite Layering

The walled of tank has layered in two modes of six-layers and three-layers of fibers with different angles and the same thickness ($t = 20 \times 10^{-3}$ m).

The finite element mesh in state of six-layer presented in Table 2 and conditions of layering of the six-layer composite are shown in Figure 6.

The finite element mesh in state of three-layer presented in Table 3 and conditions of layering of the

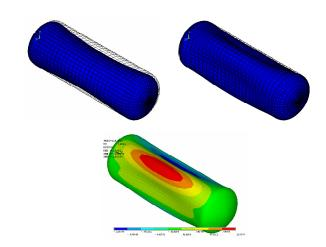


Figure 5. Axial modes of vibration of Tank.

Table 2. The finite element mesh of the six-layer composite

Element	Symmetry conditions	Fiber angle			
1263	Symmetrical	[0/30/90/90/30/0]			
222	Symmetrical	[0/45/90/90/45/0]			
234	Symmetrical	[0/60/90/90/60/0]			
245	Asymmetrical	[0/30/90/0/30/90]			
1263	Asymmetrical	[0/45/90/0/45/90]			
1325	Asymmetrical	[0/60/90/0/60/90]			
276	Asymmetrical	[15/30/45/60/75/90]			
1315	Asymmetrical	[90/75/60/45/30/15]			
1297	Symmetrical	[90/-60/30/30/-60/90]			
234	Asymmetrical balance	[90/60/30/-90/-60/-30]			
1295	Orthogonal Symmetrical	[0/90/0/0/90/0]			
269	Orthogonal Symmetrical	[0/0/0/90/90/90]			

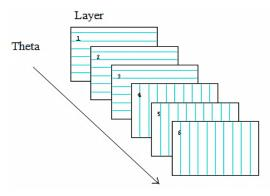


Figure 6. A View of a six-layer composite.

The finite element mesh of the three - layer Table 3. composite

Element	Symmetry conditions	Fiber angle		
253	Asymmetrical	[0/45/90]		
244	Orthogonal Symmetrical	[90/0/90]		
276	Orthogonal Symmetrical	[-90/0/-90]		
254	Symmetrical balance	[90/0/-90]		
243	Asymmetrical orthogonal	[90/0/0]		
255	Orthogonal Symmetrical	[0/90/0]		

Table 4. The natural frequencies of six-layer composite

		1		1	1					
10	9	8	7	6	5	4	3	2	1	Frequ(Hz)
										Profile
213.32	212.24	203.08	196.1	194.79	146.63	130.56	117.73	110.25	97.082	[0/30/90/90/30/0]
210.28	209.3	200.4	196.14	194.45	144.7	129.3	116.63	108.34	95.438	[0/45/90/90/45/0]
208.23	207.39	198.74	196.69	194.16	143.2	128.55	116.13	107.29	94.247	[0/60/90/90/60/0]
213.17	212.12	203.13	197.31	195.87	146.51	130.63	117.8	110.19	96.85	[0/30/90/0/30/90]
210.1	209.16	200.59	197.35	195.39	144.57	129.37	116.69	108.26	95.206	[0/45/90/0/45/90]
208.05	207.25	199.3	197.94	194.76	143.08	128.64	116.2	107.21	94.019	[0/60/90/0/60/90]
193.62	193.29	192.38	192.05	184.5	134.63	121.41	108.71	95.836	83.406	[15/30/45/60/75/90]
193.62	193.29	192.38	192.05	184.5	134.63	121.41	108.71	95.836	83.408	[90/75/60/45/30/15]
197.49	196.87	188.94	188.1	180.75	132.98	120.9	108.52	93.979	81.936	[90/-60/30/30/-0/90]
196.63	196.24	194.98	194.3	186.14	136.11	123.2	110.78	98.209	85.983	[90/60/30/-90/-60/-30]
223.73	222.58	209.7	199.22	198.18	152.66	135.91	123.33	118	102.84	[0/90/0/0/90/0]
215.82	214.9	203.3	198.57	196.94	147.43	132.2	119.95	112.94	98.079	[0/0/0/90/90/90]
		•	_							<u> </u>

Table 5. The natural frequencies of three-layer composite

10	9	8	7	6	5	4	3	2	1	Frequ(Hz) Profile
209.42	208.50	199.90	196.02	194.29	144.06	128.86	116.24	108.05	94.817	[0/45/90]
206.75	206.27	201.83	201.74	193.67	141.77	128.69	116.56	106.70	92.398	[90/0/90]
206.75	206.27	201.83	201.74	193.67	141.77	128.69	116.56	106.70	92.398	[-90/0/-90]
206.75	206.27	201.83	201.74	193.67	141.77	128.69	116.56	106.70	92.398	[90/0/-90]
223.37	222.22	209.54	198.34	197.35	152.44	135.65	123.03	117.82	102.54	[90/0/0]
223.66	222.49	209.65	198.03	197.06	152.66	135.76	123.14	117.96	102.92	[0/90/0]

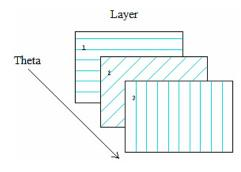


Figure 7. A View of a three-layer composite.

4. Results and Discussion

The natural frequencies with finite element and the equilibrium equations are obtained for both hypothesized model. The results of natural frequencies of the six-layer composite and three-layer composite are shown in Table 4 and Table 5.

The results in Table 4 are shown that there is no significant difference between natural frequencies in symmetrical and nonsymmetrical mode, however the symmetrical modes have higher frequencies partially. (Please see the first rows in the Table 4). The natural frequency decreased with increasing the angle of the fibers in the longitudinal direction in the symmetrical and asymmetric mode. There is no significant change in natural frequencies with increasing or decreasing of fiber angle about the x-axis in cases 7 and 8. In the state of symmetrical balance and asymmetric balance, the natural frequencies are lower than the symmetrical and asymmetric state. In orthogonal symmetrical and orthogonal asymmetric mode, the frequency is higher than previous cases and the maximum of frequency related to these modes. The lowest frequency is the state of symmetrical balance and the high frequency is of orthogonal Symmetrical.

The results in Table 4 are shown that the highest of frequency related to the orthogonal mode. Frequencies of the three modes [90/0/90], [-90/0/-90] and [90/0/-90] are equal approximately, which is reasonable because the angles 90° and -90° are identical and fiber angle placed in the same direction. The high frequency related to the orthogonal symmetrical state and the lowest frequency is of multilayer balanced state.

5. Conclusion

In this paper, vibration of horizontal cylindrical tank with different layering using the finite element method is studied. The results are as follow:

- The fiber orientation along the thickness of the tank and the number of layers affected on the natural frequency, so that with increasing the number of composite layers the natural frequency increases to some extent.
- 2. Highest frequency in cylindrical tank between three-layer and six-layer composite is in the orthogonal symmetrical modes in both layering that in the six-layer mode is more and according to the increase frequency is suitable for design of tank and the best layering for composite is with angles [0/90/0/0/90/0] in six-layer mode.
- 3. The natural frequency decreases with increase of angles in layering of the tank.
- 4. According to need, to require the high frequency range can used from both cases and considering to require the low frequency range can used the symmetrical balance mode of six-layers composite for design of tank.

Appendix. 1

Where:

$$\begin{split} k_{11} &= \int \left\{ C_{11} r \frac{\partial \psi_{i}}{\partial r} \frac{\partial \psi_{j}}{\partial r} + C_{12} \frac{\partial \psi_{i}}{\partial r} \psi_{j} + \frac{C_{11}}{r} \psi_{i} \psi_{j} \right. \\ &+ C_{12} \frac{\partial \psi_{j}}{\partial r} \psi_{i} + C_{66} r \frac{\partial \psi_{i}}{\partial z} \frac{\partial \psi_{j}}{\partial z} \right\} dr \, dz \\ k_{12} &= k_{21} = \int \left\{ C_{12} r \frac{\partial \psi_{i}}{\partial r} \frac{\partial \psi_{j}}{\partial z} + C_{12} \frac{\partial \psi_{j}}{\partial z} \psi_{i} + \frac{C_{11}}{r} \psi_{i} \psi_{j} \right. \\ &+ C_{12} r \frac{\partial \psi_{j}}{\partial r} \psi_{i} + C_{66} r \frac{\partial \psi_{i}}{\partial z} \frac{\partial \psi_{j}}{\partial r} \right\} dr \, dz \end{split} \tag{11}$$

$$k_{22} &= \int \left\{ C_{66} r \frac{\partial \psi_{i}}{\partial r} \frac{\partial \psi_{j}}{\partial r} + C_{11} r \frac{\partial \psi_{i}}{\partial z} \frac{\partial \psi_{j}}{\partial z} \right\} dr \, dz \\ F_{1} &= \left[\iint \psi_{i} t_{r} ds, \ F_{2} = \left[\iint \psi_{i} t_{z} ds, \ Q_{1} = \int (r \frac{\partial \psi_{i}}{\partial r} + \psi_{i}) \sigma_{T} \, dr \, dz, \right. \\ Q_{2} &= \int \frac{\partial \psi_{i}}{\partial z} \sigma_{T} r \, dr \, dz \end{split}$$

And

$$\psi_1 = \left(1 - \frac{r}{a}\right)\left(1 - \frac{z}{b}\right), \psi_2 = \frac{r}{a}\left(1 - \frac{z}{b}\right), \psi_2 = \frac{z}{b}\left(1 - \frac{r}{a}\right), \psi_2 = \frac{r}{a}\frac{z}{b}$$
(12)

6. References

- Damatty AA El, Korol RM, Mirza FA. Stability of elevated liquid-filled conical tanks under seismic loading, part i-theory. Earthquake Eng Struct Dynam. 1997; 26:1191–208.
- Mansouri A, Aminnejad B. Investigation of oil reservoir vibration under the impact of earthquake in proper and corrosion-occurred tanks. Am J Civ Eng Architect. 2013; 1(6):181–99.
- 3. Sweedan AMI, Damatty AA El. Experimental identification of the vibration modes of liquid-filled conical tanks and validation of a numerical model. Earthquake Eng Struct Dynam. 2003; 32:1407–30.
- 4. Amabili M. Nonlinear vibrations of circular cylindrical shells with different boundary conditions. AIAA Journal. 2003; 41:1119–30.
- 5. Amabili M. Theory and experiments for large-amplitude vibrations of empty and fluid-filled circular cylindrical shells with imperfections. J Sound Vib. 2003; 262:921–75.

- 6. Amabili M. Comparison of different shell theories for large-amplitude vibrations of empty and fluid-filled circular cylindrical shells with and without imperfections: lagrangian approach. J Sound Vib. 2003; 264:1091-25.
- 7. Karagiozis KN, Amabili M, Paidoussis MP, Misraa AK. Nonlinear vibrations of fluid-filled clamped circular cylindrical shells it. J Fluid Struct. 2005; 21:579-95.
- 8. Zhou D, Liu W. Hydro elastic vibrations of flexible rectangular tanks partially filled with liquid. Int J Numer Meth Eng. 2006; 71(2):149-74.
- 9. Dehghan Manshadi SH, Maheri Mahmoud R. The effects of long-term corrosion on the dynamic characteristics of

- ground based cylindrical liquid storage tanks. Thin-Walled Structures. 2010; 48: 888-96.
- 10. Pal NC, Bhattacharyya SK, Sinha PK. Non-linear coupled slosh dynamics of liquid-filled laminated composite containers: a two dimensional finite element approach. J Sound Vib. 2003; 261:729-49.
- 11. Larbi W, Deu JF, Ohayon R. Vibration of ax symmetric composite piezo electric shells coupled with internal fluid. Int JNumer Meth Eng. 2007; 71(12):1412-35.
- 12. Moslemi M, Kianoush M R. Parametric study on dynamic behavior of cylindrical ground-supported tank. Eng Struct. 2012; 42:214-30.